Optical and X-ray Emission Spectroscopy of High-Power Laser-Induced Dielectric Breakdown in Molecular Gases and Their Mixtures

Dagmar Babánková,[†,‡] Svatopluk Civiš,[*,†] Libor Juha,[‡] Michal Bittner,[‡] Jaroslav Cihelka,[†,‡] Miroslav Pfeifer,[‡] Jiří Skála,[‡] Andrzej Bartnik,[§] Henryk Fiedorowicz,[§] Janusz Mikolajczyk,[§] Leszek Ryć,[||] and Tereza Šedivcová[^]

J. Heyrovský Institute of Physical Chemistry, Czech Academy of Sciences, Dolejškova 3, 182 23 Prague 8, Czech Republic, Institute of Physics, Czech Academy of Sciences, Na Slovance 2, 182 21 Prague 8, Czech Republic, Institute of Optoelectronics, Military University of Technology, ul. Kaliskiego 2, PL-00-908 Warsaw, Poland, Institute of Plasma Physics and Laser Microfusion, ul. Hery 23, PL-00-908 Warsaw, Poland, and Institute of Organic Chemistry and Biochemistry, Czech Academy of Sciences, Flemingovo nam. 2, 166 10 Prague 6, Czech Republic

Received: June 13, 2006; In Final Form: August 17, 2006

Large-scale plasma was created in molecular gases (CO, CO_2, N_2, H_2O) and their mixtures by high-power laser-induced dielectric breakdown (LIDB). Compositions of the mixtures used are those suggested for the early earth's atmosphere of neutral and/or mildly reducing character. Time-integrated optical spectra emitted from the laser spark have been measured and analyzed. The spectra of the plasma generated in the CO-containing mixtures are dominated by emission of both C_2 and CN radicals. A vibrational temperature of $\sim 10^4$ K was determined according to an intensity distribution in a vibronic structure of the CN ($B^2\Sigma^+_u - X^2\Sigma^+_g$) violet band. For comparison, the $NH_3-CH_4-H_2-H_2O$ mixture has been irradiated as a model of the strongly reducing version of the early earth's atmosphere. In this mixture, excited CN seems to be significantly less abundant than C_2. The LIDB experiments were in the molecular gases carried out not only in the static cell but also using a large, double stream pulse jet (gas puff target) placed in the vacuum interaction chamber. The obtained soft X-ray emission spectra indicate the presence of highly charged atomic ions in the hot core of high-power laser sparks.

I. Introduction

Both electrical discharge[1−4] and laser-produced[4−7] plasmas have been used for an initiation of abiotic synthesis of organic molecules in mixtures of molecular gases simulating early earth's and other planetary atmospheres. These plasmas serve as a laboratory model of atmospheric high-energy density events, such as atmospheric discharges (i.e., lightning)[8,9] and impact of extraterrestrial bodies (i.e., comets and meteorites),[10] and their role in chemical evolution. Particular plasmas of both kinds[3,8] have already been investigated on how their characteristics fit properties of real lightning and impact plumes. The optical emission spectroscopy (OES)[11−14] represents the plasma diagnostic method frequently used for these purposes.[3,8] This simple method provides information not only on an abundance of excited species and course of excitation processes occurring in the plasma but also on basic plasma characteristics (e.g., its temperature). Thus, the OES data help not only to shed light on mechanisms of organic molecules formation under the given conditions but provide information also on relevance of the small-scale laboratory plasma to the real, large-scale atmospheric events.

OES has frequently been used for the study of chemical consequences of laser-induced dielectric breakdown (LIDB) in various molecular gases.[15−19] The method has already demonstrated its ability to provide information on radiating LIDB plasma composition and temperature, required for gaining knowledge about the mechanisms of the laser plasma chemical processes. In addition to that, OES data obtained with small, high-repetition lasers can be compared with the data reported in this article for the high-power laser system to evaluate parameter differences of chemically active plasmas formed in these two ways.

The laser pulse energy deposited in the LIDB plasma can be transferred to the surrounding gas to initiate there a chemical change through (a) short-wavelength radiation (i.e., UV−VUV/XUV radiation and X-rays) and energetic charged particles emitted from the hot plasma core, (b) a shock wave created by LIDB, and (c) mixing and interaction of the plasma containing huge amounts of highly reactive species (atoms, atomic and molecular ions, free radicals) and thermal waves propagating through the gas.

The roles these processes play within real LIDB plasmas are determined by the laser pulse characteristics controlling both the electron temperature and other plasma parameters and their ability to initiate particular chemical reactions in a given

* Corresponding author. Phone: +420-266053275. Fax: +420-286591766. E-mail: civis@jh-inst.cas.cz.
† J. Heyrovský Institute of Physical Chemistry, Czech Academy of Sciences.
‡ Institute of Physics, Czech Academy of Sciences.
§ Military University of Technology.
|| Institute of Plasma Physics and Laser Microfusion.
^ Institute of Organic Chemistry and Biochemistry, Czech Academy of Sciences.

10.1021/jp063689o CCC: $33.50
Published on Web 10/12/2006

molecular system. On the other hand, the particular processes are distinguished in both time and space. Therefore, by bringing a spatial and time resolution to emission spectroscopy of the LIDB plasmas, we may investigate relationships between the physical processes and chemical action connected to a laser spark.

In this article, an overall optical emission of high-power laser-induced dielectric breakdown in various molecular gases and their mixtures has been measured and analyzed. Such a plasma was also generated in a gas plume provided in the vacuum interaction chamber by a pulsed gas jet (i.e., gas puff). In addition to the optical spectroscopy, X-ray emission was studied in the dynamic version of the LIDB experiments.

II. Experimental Section

Laser-induced dielectric breakdown in the molecular gases was achieved with a high-power iodine photodissociation laser system, the Prague Asterix Laser System (PALS).[20] A single pulse of radiation with a wavelength of 1.3152 μm (pulse duration of 400 ps and energy of hundreds of Joules) was extracted behind either the fourth or fifth amplifier of the system. The laser beam had a diameter of 15 and 29 cm behind the fourth and fifth amplifier, respectively. One pulse was delivered every 25 min.

The fourth amplifier beam was focused into a gas cell by a planoconvex lens, with a diameter of 15 cm and focal length of 25 cm. Pulse energy losses at the focusing lens and cell window did not exceed 15%.

The 15-L glass cell used in the static LIDB experiments is shown in Figure 1a. The cell's body had a shape of a cross with both length and width of 40 cm. There were four windows. The main, laser-beam entrance windows were made of 4-cm-thick glass and had a diameter of 20 cm. Inspection windows 1.5-cm thick and 10 cm in diameter served for collecting the OES signals. The windows were connected to the glass body by stainless steel flanges and sealed with viton rings. The cell was mounted on a 1-cm-thick aluminum plate, making possible its easier manipulation and positioning. The cell body was equipped with two vacuum valves (ACE Glass) for gas handling. The complete glass cell setup weighed about 70 kg.

Before every experiment, the cell was disassembled, cleaned, and heated to 450 °C inside an oven. Then the cell was evacuated to a pressure of 3×10^{-5} Torr and filled with high purity N_2, CO, CO_2, H_2, NH_3, and/or CH_4 gases up to atmospheric pressure. Under the flow of such gas mixture, 20 mL of deionized water was added into the cell. The filled cell was then closed and transported to the laser facility.

Double-stream gas puff targets utilized two coaxial nozzles,[21] as depicted in Figure 1b. The gas plume was formed in the nozzle by pulsed injection of pressurized gas from an electromagnetic valve. The outer nozzle orifice was a ring with outer and inner diameters of 3.0 and 2.5 mm, respectively. The annular outer nozzle produced a hollow cylinder of helium, suppressing sideways expansion of investigated molecular gases. The full 29-cm beam, extracted from the PALS after fifth amplifier, was focused into the gas puff. Laser pulse energies were varied from 100 to 600 J. Soft X-ray emission spectra were measured with a transmission grating spectrometer (4000 lines/mm) and recorded by the back illuminated CCD42-40 camera (Marconi).

In the glass cell case, one of the glass windows perpendicular to the laser beam was used for the emission spectroscopy measurements. Radiation was collected by glass lens and focused on the entrance slit of the spectrometer. Two ruled gratings were switched in the spectrometer (MS257, Oriel), one

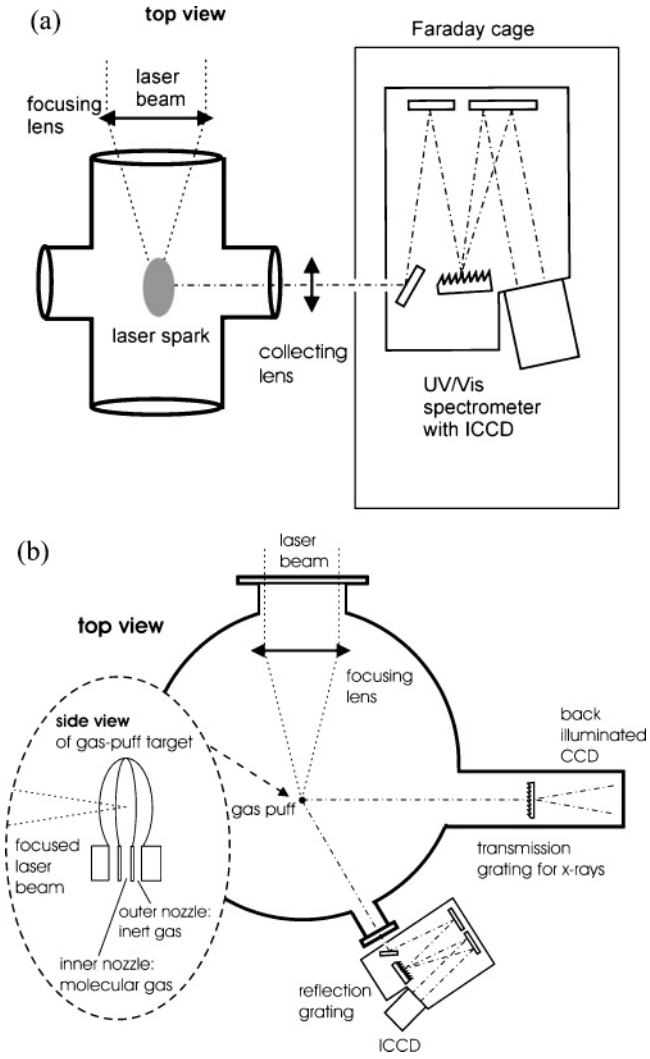

Figure 1. Static (a) and dynamic (b) layouts for spectroscopic investigation of large laser sparks. Top view, not to scale.

for preview (150 lines/mm, width of measured spectra = 400 nm) and the second for a high-resolution measurement (1200 lines/mm, width of measured spectra = 60 nm). The dispersed spectrum was detected by intensified CCD camera (ICCD; iStar 720, Andor), with a resolution of 0.08 nm/pixel for the high-resolution grating. Spectral lines in a distance down to 0.2 nm were distinguished if a very narrow entrance slit was used.

The synchronization of intensified CCD camera with the laser pulse was accomplished using a signal from the photodiode. Spectrum was integrated for the time of 5 s after the trigger. Each spectrum presented here corresponds to gas exposure with a single laser shot.

In the case of the gas puff, LIDB plasma was observed with the same spectrometer through a window in the wall of the vacuum interaction chamber. No focusing lens was used.

Both experimental layouts can be seen in Figure 1. Because of jeopardy of an electrical interference on the ICCD head occurring in the high-power laser hall, the spectrometer was placed in the Faraday cage.

III. Results

A. Optical Emission from the Gas Cell. *Carbon Monoxide.* All our spectra were integrated over the whole period of LIDB plasma formation, expansion, and recombination and over a radiating surface of the large LIDB fireball formed by high-

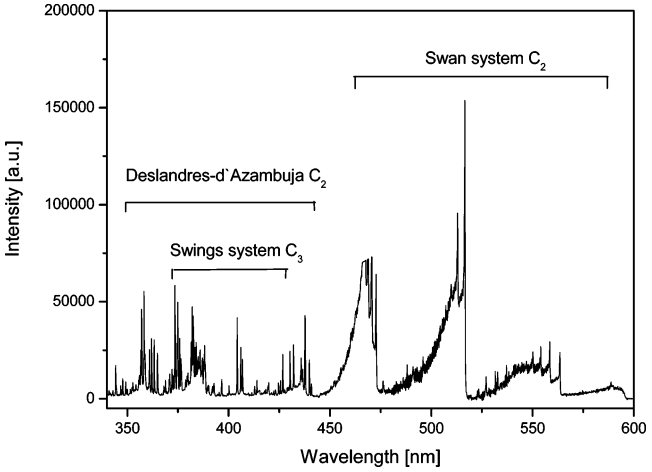

Figure 2. Optical emission spectrum of LIDB in carbon monoxide gas.

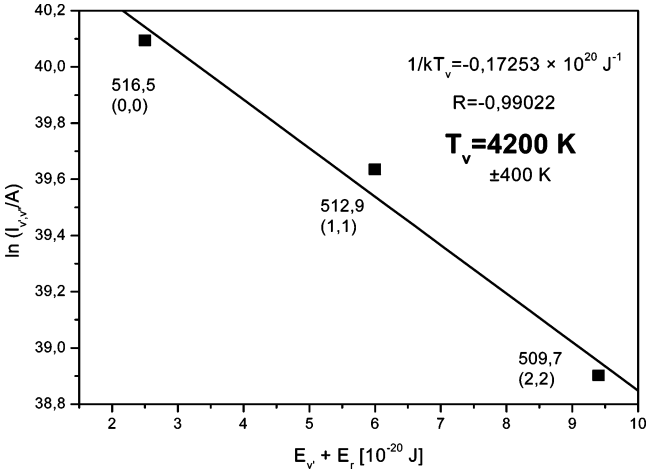

Figure 3. Determination of the vibrational temperature using the slope of the Boltzmann plot. The vibrational sequence of $\Delta v = 0$ of the C_2 Swan band was used.

power laser. The optical spectrum taken in the atmospheric pressure CO gas is shown in Figure 2, and assignment of the emission lines is in Table 1 of the Supporting Information. The measured spectra are mostly composed of molecular emission spectra of C_2 and C_3 radicals and atomic and atomic ion lines of C and O. The Swan system of C_2 ($D^3\Pi_g - A^3\Pi_u$) dominates in our spectra in the spectral interval between 450 and 550 nm.[22−29] In addition, some lines belonging to the Swings band of C_3 ($A^1\Pi_u - X^1\Sigma_g$) appeared at 380−420 nm.[22,27,30,31] This band is partly overlapped with Deslandres-D'Azambuja C_2 band ($C^1\Pi_g - A^1\Pi_u$) at 350−410 nm.[22,23,28]

There are five Swan bandheads in the $\Delta v = -2, -1, 0, 1,$ and 2 sequences in the spectrum. At 358 and 385 nm, two quite weak bands appeared belonging to the CN radical violet system ($B^2\Sigma^+_u - X^2\Sigma^+_g$). It is probably caused by the presence of small leaks or some impurities of nitrogen in the pressure bottle.

The vibrational temperature of gaseous mixtures was determined by the relative vibrational population of $\Delta v = 0$ sequence of C_2 radical with the following equation:[32,33]

$$I_{v'v''} = C\nu_h^4 p(v',v'')J_h\Delta J \exp\left[-\frac{E_{v'} + hcB_{v'}J_h(J_h - 1)}{kT}\right] \quad (1)$$

where $I_{v'v''}$ is the bandhead intensity, C is constant, ν_h is bandhead wavelength, $p(v',v'')$ is the probability of vibrational transition, J_h is the rotational quantum number, ΔJ represents the number of distinguished lines in the head of the band, $E_{v'}$ is the vibrational energy of upper electronic level, and $B_{v'}$ is the rotational constant. If $\ln I_{v'v''}/[p(v',v'')\nu_h^4 J_h \Delta J]$ is plotted as a function of $E_{v'} + E_{R(v')}$, where $E_{R(v')} = hcB_{v'}J_h(J_h - 1)$, and the Boltzmann distribution of the vibrational energies is preserved, then the slope of the obtained line can be used to determine the temperature. For this purpose, the rotational temperature was determined from the ratio of the normalized intensity of the (0,0) C_2 Swan band at 516.5 nm and local maximum between 516 and 513.5 nm.[34]

The estimated vibrational temperature was about 4200 K (Figure 3), and the rotational temperature was about 4500 K. The almost identical values of both temperatures indicate local thermodynamic equilibrium (LTE) of formed plasma.

Molecular Nitrogen. The LIDB spectrum of N_2 at pressure of 350 Torr can be seen in Figure 4. The spectrum is composed of one broad band. This band in spectral region 300−700 nm is created from unresolved lines of single charged nitrogen ion and probably from electronic transition $B^2\Sigma_u^+ - X^2\Sigma_g^+$ of 0−0 first negative band of N_2^+. The experimentally recorded

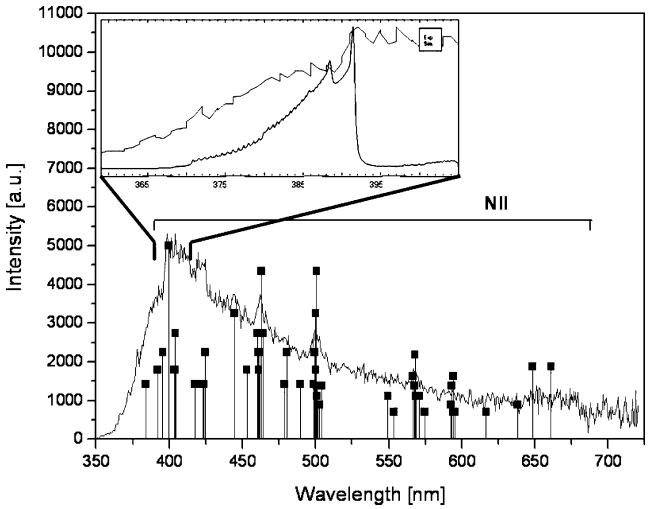

Figure 4. Optical emission spectrum of LIDB in nitrogen compared with atomic lines of N^+ and simulated $B^2\Sigma_u^+ - X^2\Sigma_g^+$ electronic transitions of 0−0 band of N_2^+ using the simulation program LIFBASE[35] and molecular parameters taken from ref 36.

spectrum is compared with the predicted spectrum in a spectral range of 380−400 nm for temperature 4200 K and resolution of 1 nm.

Water Vapor. The laser plasma cell was evacuated and filled with water vapor to a pressure of 20 Torr, which is a partial pressure of water at 20 °C. Its LIDB spectrum is shown in Figure 5, and assignment of the emission lines is in Table 2 of the Supporting Information. The spectrum is dominated by the H_α, H_β, H_γ, H_δ, and H_ϵ lines of the atomic hydrogen Balmer series in a spectral interval between 400 and 700 nm. In the near-infrared region, we observed lines of atomic oxygen at 777.5, 820.4, and 844.6 nm. The remaining lines are second orders of H_δ, H_γ and H_β.

The excitation temperature was determined from the relative intensities of atomic hydrogen lines of the Balmer series with the following equation:[37,38]

$$\ln\left(\frac{I_i.\lambda_i}{g_i.A_{ij}}\right) = -\frac{E_i}{k.T_{ex}} + C \quad (2)$$

where I_i is the relative line intensity, λ_i is the wavelength, g_i is the statistical weight, A_{ij} is Einstein's coefficient of spontaneous emission, and E_i is the energy of upper electronic level. The

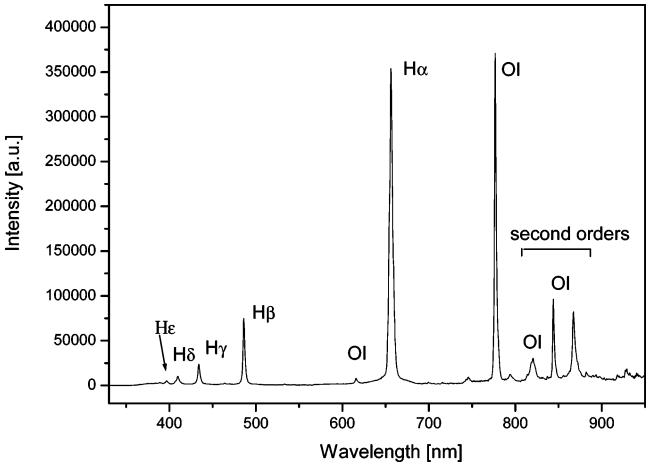

Figure 5. Optical emission spectrum of LIDB in water vapor.

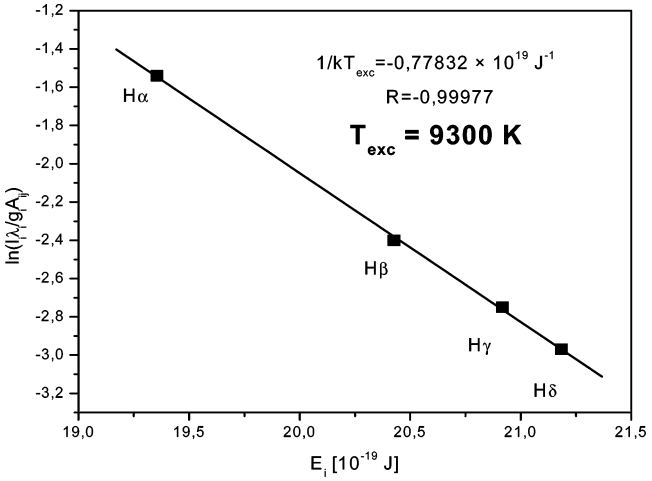

Figure 6. Determination of excitation temperature from Balmer series of hydrogen atoms.

slope of the line $\ln(I_i.\lambda_i/g_i.A_{ij})$ versus E_i yields the value of the excitation temperature. The estimated excitation temperature was 9300 K (Figure 6).

This temperature very well approaches temperatures if hydrogen atoms are excited due to inelastic collisions with free electrons.[37,38]

$CO-N_2-H_2O$ Gas Mixture. The spectrum was collected at atmospheric pressure over the spectral range 340−800 nm (Figure 7). Figure 8 shows the LIDB emission spectra in the UV spectral region. Assignment of the emission lines in the $CO-N_2-H_2O$ mixture is in Table 3 of the Supporting Information. Its LIDB emission spectrum is dominated by a strong band from the CN radical, specifically the electronic transition $B^2\Sigma^+_u-X^2\Sigma^+_g$.[22,28,39−42] There are three sequences in the spectrum: $\Delta v = 1$ in the 358 nm region, $\Delta v = 0$ in the 388 nm region, and $\Delta v = -1$ in the 415 nm region. These sequences appear in the spectrum as second orders as well. Swan bands of the C_2 radical electronic transition $D^3\Pi_g-A^3\Pi_u$ were identified in a spectral range around 470 nm. There are vibrational transitions with $\Delta v = 2$ in the 437 nm region, $\Delta v = 1$ in the 469 nm region, and $\Delta v = 0$ in the 512 nm region. In addition to CN and C_2 bands, there are lines from neutral and ionized carbon, oxygen, and nitrogen atoms in the spectrum. The atomic and atomic ion lines dominated in the short wavelength spectral region (Figure 8)

Intensified CCD allowed us to investigate temporal evolution of the CN violet band. Time-resolved spectra were measured by changing an integration time of the detector from 1 μs to 1 s. The spectra are shown in Figure 9. The measured spectra depict that the first 3 μs after the laser spark dominates in the spectrum a broad background continuum due to bremsstrahlung radiation from electron−ion collisions. No atomic or atomic ion lines have been observed. The CN radical starts to be formed 4 μs after the laser pulse.

We were able to determine vibrational temperature from the $\Delta v = 0$ sequence of the CN violet band. The obtained value of

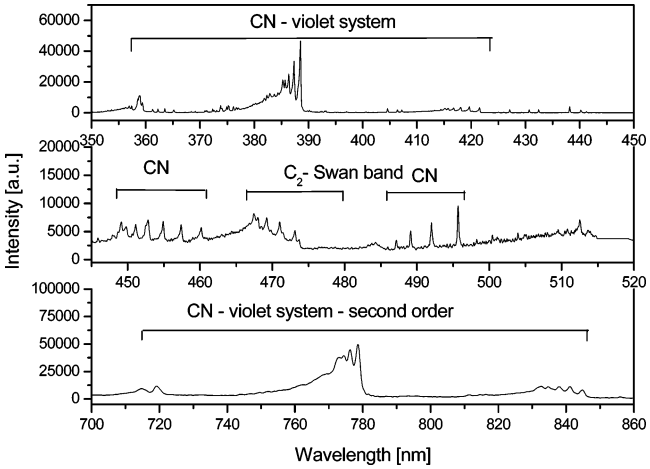

Figure 7. Optical emission spectrum of LIDB in the $CO-N_2-H_2O$ gas mixture.

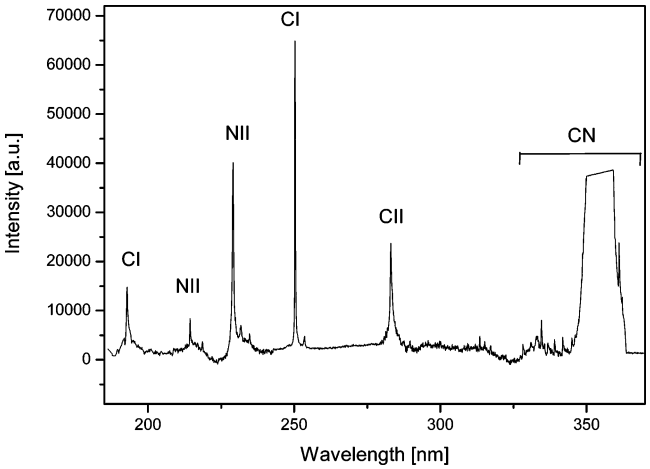

Figure 8. Ultraviolet emission spectrum of LIDB in the $CO-N_2-H_2O$ gas mixture.

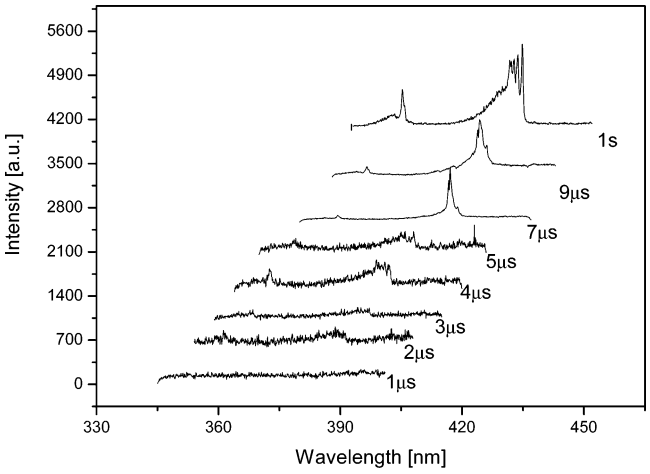

Figure 9. Temporal evolution of optical emission spectra taken from the LIDB plasma created by 100 J laser pulse focused into the $CO-N_2-H_2O$ mixture in the glass cell.

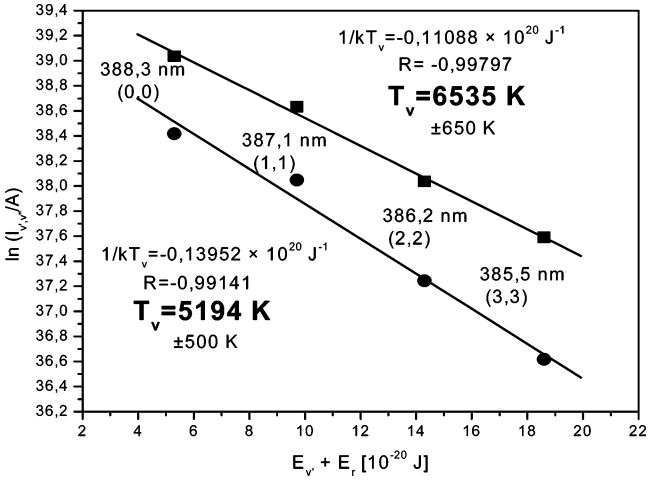

Figure 10. Determination of the vibrational temperature of the mixture $CO-N_2-H_2O$ (■) and $CO-N_2-H_2O-Xe$ (●) using the Boltzmann plot and the $\Delta v = 0$ sequence of the CN violet band.

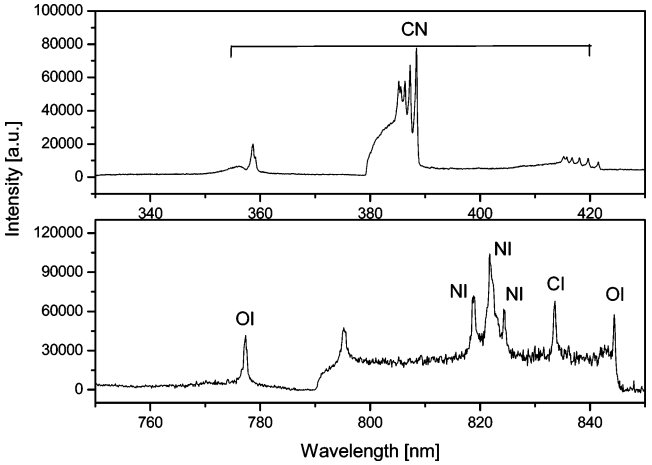

Figure 11. Optical emission spectrum of LIDB in the $CO_2-N_2-H_2O$ gas mixture.

the vibrational temperature was about 6535 K (Figure 10). This gaseous mixture was investigated in two more modifications: with higher partial pressure of water vapor (higher temperature) and with the 12% of xenon in the mixture. Excited ions of Xe de-excite easily by loosening the quanta of short wavelength radiation (∼keV).[43] Therefore, the role of short wavelength radiation for transport of the energy into the surrounding area can be studied by adding the Xe into the reaction mixture. Nevertheless, there were no qualitative differences between the spectra of mixtures containing Xe and free of Xe. The estimated vibrational temperature for the Xe-containing mixture was 5194 K (Figure 10) and the Xe-free $CO-N_2-H_2O$ mixture showed slightly higher temperature that reflected the role of xenon as a buffer gas.

$CO_2-N_2-H_2O$ Gas Mixture. Surprisingly, the CO_2-based mixture emits just CN bands. In contrast to the CO-containing mixture, C_2 emission has not been observed (Figure 11). Assignment of the emission lines is in Table 4 of the Supporting Information. An absence of NO emission in the LIDB spectrum was an interesting fact because NO is usually formed by spark discharge in CO_2-N_2 rather then HCN.[44] The vibrational temperature 6169 K (Figure 12) was estimated from the sequence of $\Delta v = 0$ of CN radical, which is in good agreement with the value of vibrational temperature obtained in the mixture $CO-N_2-H_2O$ under the same conditions.

$NH_3-CH_4-H_2O-H_2$ Gas Mixture. Methane-based mixture has been irradiated as a model of the strongly reducing early

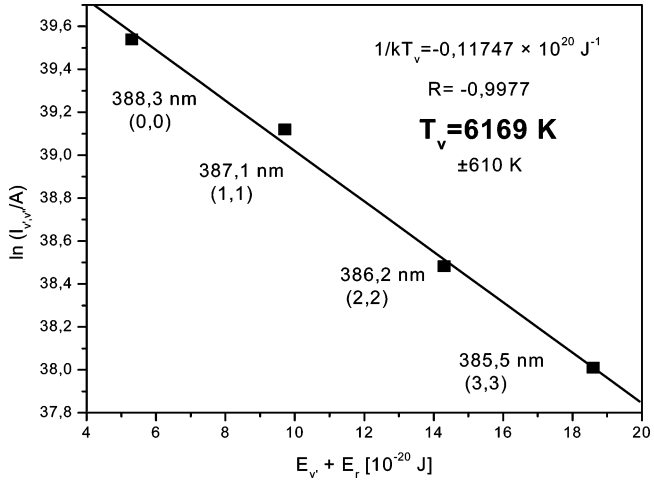

Figure 12. Determination of the vibrational temperature for the $CO_2-N_2-H_2O$ mixture using the Boltzmann plot method. To calculate the intensity of the vibrational sequence $\Delta v = 0$ of CN radical was used.

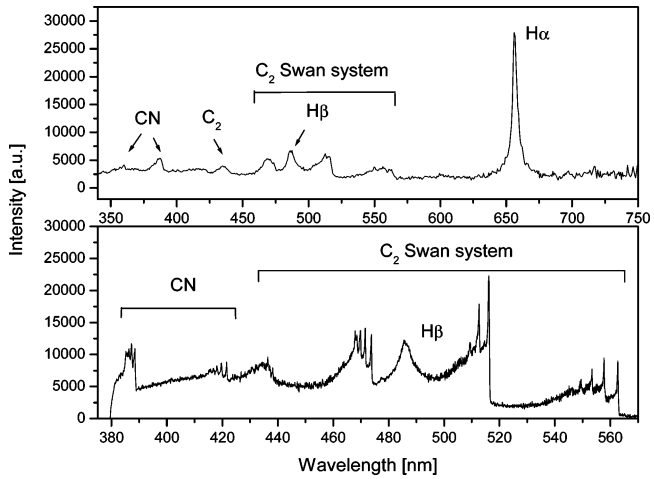

Figure 13. Optical emission spectrum of LIDB in the $NH_3-CH_4-H_2-H_2O$ gas mixture.

earth's atmosphere as suggested and investigated by Urey and Miller, respectively.[1,2] In contrast to the carbon monoxide-based mixtures, the excited CN seems to be less abundant than C_2 in the LIDB plasma created from the $NH_3-CH_4-H_2O-H_2$ mixture (Figure 13). Assignment of the emission lines is in Table 5 of the Supporting Information.

All three types of temperature were determined in this mixture. The vibrational temperature, determined from the $\Delta v = 0$ sequence of C_2 radical, was 8050 K (Figure 14); the excitational temperature, determined from the relative intensities of atomic hydrogen lines, was 8100 K (Figure 15); and the rotational temperature was 8300 K. This fact demonstrates the validity of LTE approximation.

The electron density in the LIDB plasma was determined using the method based on the Stark broadening of the H_β spectral line spontaneously emitted by the plasma.[45] In this investigation, the Voigt function was fitted to the measured H_β line profile to estimate the full width at half-maximum (FWHM) of the Lorentzian (Stark) profile $\Delta\lambda^{Stark}(H_\beta)$ (Figure 16). The simple relation for n_e used by Goktas et al.[46] for electron temperature in the range of 1−4 eV and electron density between 10^{14} and 10^{18} cm^{-3} is

$$n_e = 1.09 \times 10^{16}[\Delta\lambda^{Stark}(H_\beta)]^{1.458}[\text{cm}^{-3}] \qquad (3)$$

where $\Delta\lambda^{Stark}(H_\beta)$ is expressed in nm. The resulting value of

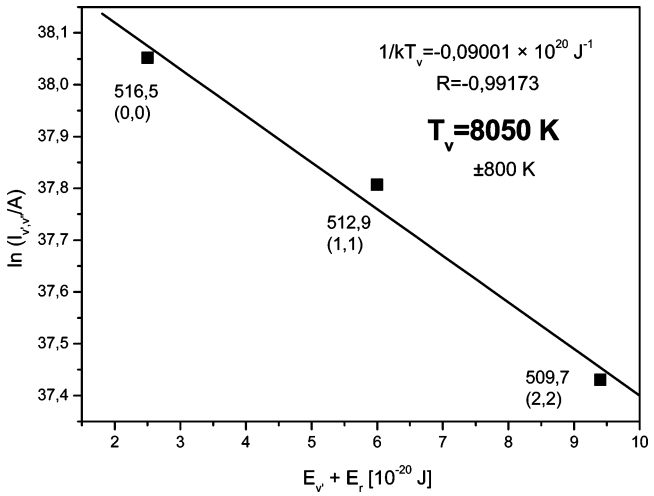

Figure 14. Determination of the vibrational temperature for the $NH_3-CH_4-H_2-H_2O$ mixture using the slope of the Boltzmann plot. To calculate the intensity of the vibrational sequence $\Delta v = 0$ of the Swan band of C_2 radical was used.

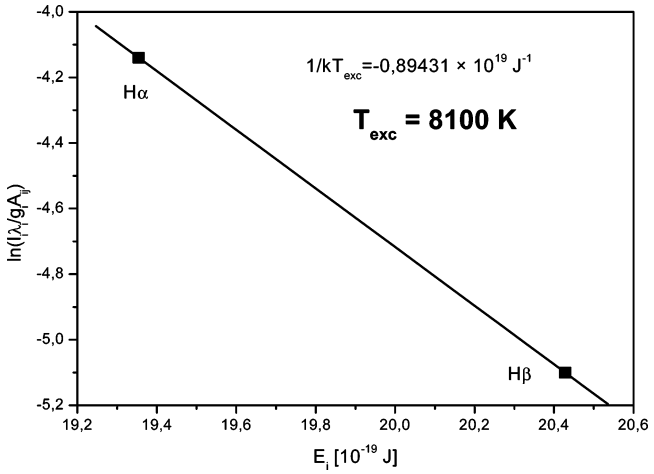

Figure 15. Determination of the excitational temperature from the relative intensities of atomic hydrogen lines H_α and H_β of the Balmer series.

the FWHM of the Lorentzian profile $\Delta\lambda^{\text{Stark}}(H_\beta) = 6.13$ nm yields the value of electron density $n_e = 1.53 \times 10^{17}$ cm^{-3}.

Bekefi[47] and McWhirter[48] have derived a necessary (but not sufficient) criterion for LTE:

$$n_e \geq 1.4 \times 10^{14} T_e^{1/2} (\Delta E_{mn})^3 [\text{cm}^{-3}] \qquad (4)$$

where T_e is electron temperature in eV and ΔE_{mn} is energy difference between the upper and lower energy levels (in eV). Substituting values for T_e (0.7 eV) and ΔE (2.5 eV) in eq 4, we find that the lowest limit for n_e is 1.9×10^{15} cm^{-3}. Our calculated values of n_e are much greater than this limit, implying the validity of LTE approximation.

B. Optical and X-ray Emission from the Pulse Gas Jet (Gas Puff). A significant difference has been found in the optical spectra of LIDB plasmas created in CO- and N_2-containing mixtures in the static cell and gas puff. In the case of the jet, there is no examined emission from molecular species (Figure 17). It demonstrates that new molecules are formed in the phase of laser spark evolution where the LIDB plasma expands into the surrounding gas. Such a period does not take place in the gas puff because the LIDB plasma expands through the thin layer of helium directly into vacuum.

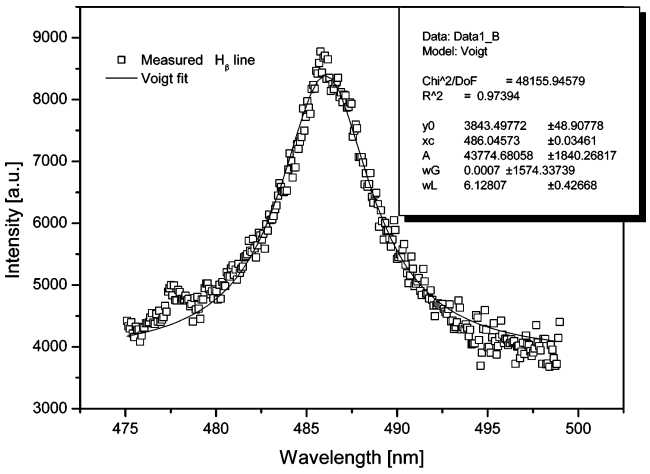

Figure 16. Measured H_β line profile and the Voigt function fit.

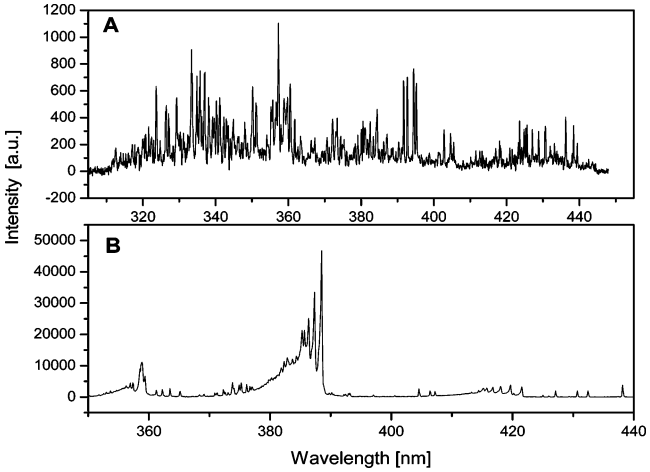

Figure 17. Comparison of the LIDB emission spectra measured in the gas puff filled with (a) $CO-N_2$ together with (b) $CO-N_2-H_2O$ mixture in the static cell.

Short-wavelength emission spectra collected in Figure 18 testify to a high abundance of highly charged ions (N^{6+}, O^{7+}, C^{4+}, etc.) and strong XUV/X-ray emission from the hot core of high-power laser sparks. It is clear that the high-power LIDB plasma itself, before its expansion into a cold molecular gas, has a high electron temperature and its chemical action can only be destructive (i.e., molecules are decomposed into atoms and atomic ions).

Experiments with the gas puff provide the unique ability to look through the vacuum and inert, weakly absorbing gases (here He) and observe the short-wavelength emission of LIDB plasma. This cannot be done in the static cell due to strong absorption of short-wavelength radiation in the cold, dense gas. It is expected that short-wavelength radiation could play a significant role in the chemical action of LIDB plasmas, initiating photochemical and/or radiation-chemical reactions in the surrounding gas.

IV. Discussion

The purpose of this work was to determine whether large laser sparks might be used to synthesize simple organic molecules, which participated in the formation of life on the early earth, from simple inorganic gases (CO, CO_2, H_2O, CH_4, NH_3, and N_2).

Laser-induced dielectric breakdown was realized with a laser pulse of energy <1 kJ in mixtures of molecular gases represent-

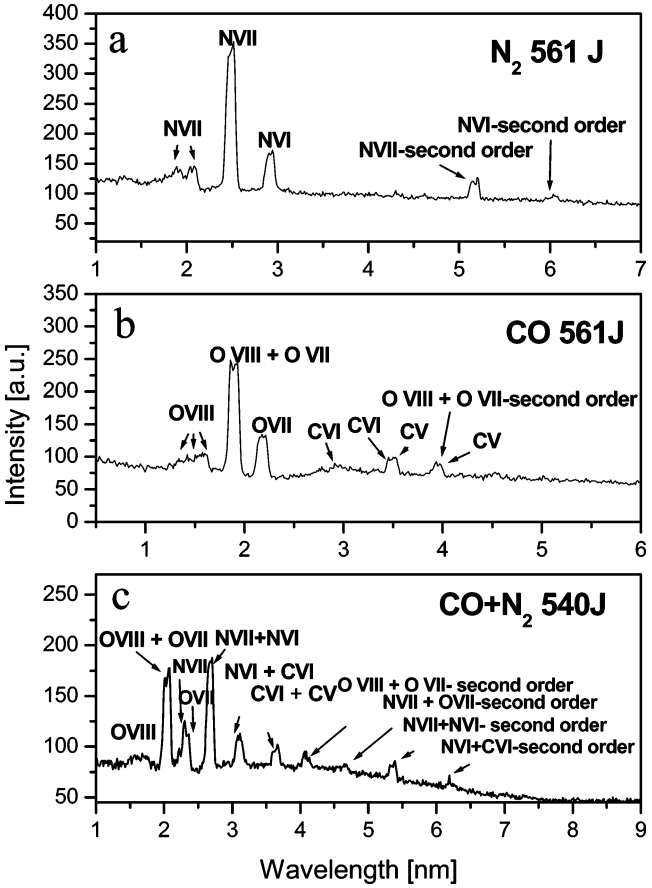

Figure 18. Soft X-ray emission spectra of laser sparks from pulse jet experiments: (a) N_2, (b) CO, and (c) $CO-N_2$.

ing various compositions of the original atmosphere of the earth. A PALS iodine photodissociation laser, working at a basic wavelength of 1315 nm, providing short, 0.5-ns laser pulses with an energy of up to 1 kJ, was used for this purpose. At the given length of the pulse, the high-energy content corresponds to high intensity. If such a beam is focused in a gas mixture, a LIDB threshold is achieved at a substantially greater distance from the focal point, where the diameter of the beam is much greater. Thus, a high-power, 100 J pulse can produce an order of magnitude greater volume of LIDB plasma than the laser pulses with energies of $\sim 0.1-1$ J used to date.

Until now, these experiments were carried out using small lasers with high-repetitive frequencies, yielding low-energy pulses or electric discharges. Large laser sparks could be a better laboratory instrument simulating processes with high-energy intensity, such as lightning discharges or the impact of an extraterrestrial body into the earth's atmosphere. In these atmospheric processes, the hot plasma is separated to a substantial degree in space and time from the final products of the reactions that it initiates in the atmospheric gases. Pulses with high-energy content permit fulfilling of this condition. Several high-energy laser pulses can be used to deposit the same amount of energy in a gas mixture as thousands of low-energy pulses; however, it is possible to avoid the undesirable action of subsequent laser pulses on the already-formed products, which is unavoidable with low-energy pulses. When the laser pulse has sufficient energy, such an experiment can theoretically be carried out with a single pulse and thus simulate in the laboratory a time-limited high-energy event.

Processes leading to the formation of organic molecules were monitored in three ways. These consisted of indication and determination of stable products in the liquid phase using highly sensitive instrumental analytical techniques (high-performance liquid chromatography with a mass spectrometer detector),[7] detection of unstable species on the principle of optical and X-ray emission spectroscopy (this work), and finally, monitoring changes in the composition of the gas phase by high-resolution Fourier transform IR spectrometry and gas chromatography (to be published).

In addition to conventional experiments in a static glass cell, measurements were carried out with a pulse jet, which provided a unique opportunity to study the LIDB plasma in the initial stages of its development and monitor short-wave radiation in the extreme ultraviolet (XUV) and soft X-ray spectral regions, emitted by the plasma, which were absorbed by the cold gas molecules surrounding the spark under conventional, static conditions.

V. Conclusions

Laser emission spectroscopy was used to monitor unstable particles formed by the action of large laser sparks in gas mixtures of various compositions. Molecular emission bands dominated in all the emission spectra. The $CO-N_2-H_2O$ mixture contained the bands of C_2 radicals (Swan and Deslandres-D'Azambuja systems), the C_3 radical (Swings system), and the CN radical (violet system). Only bands belonging to the CN radical (violet system) were found in the $CO_2-N_2-H_2O$ mixture. The bands of the C_2 radical (Swan system) predominated in the $NH_3-CH_4-H_2-H_2O$ mixture, with less intense bands of the CN radical (violet system). Two very strong lines of atomic hydrogen H_α and H_β were identified in this mixture. The identified molecular bands were used for determination of the parameters of the plasma formed.

The vibration temperature was determined from the slope of the Boltzmann line. The calculation was carried out on the basis of the $\Delta v = 0$ CN sequence and C_2 radicals. The rotation temperature was determined from the ratio between the standard intensity of the head of the (0,0) bands of the C_2 radical at 516.5 nm and the local maximum in the 516−513.5 nm region, that is, between the (0,0) and (1,1) vibration lines of the C_2 Swan band. The excitation temperature could be determined for the $NH_3-CH_4-H_2-H_2O$ mixture and for water vapors from the relative intensities of the hydrogen atomic lines of the Balmer series. The values of the individual temperatures for the given gas mixture were in very good agreement, indicating that the system was in local thermodynamic equilibrium. The vibration temperature of carbon monoxide alone had a value of 4200 K. The values of the vibration temperatures of the $CO-N_2-H_2O$ and $CO_2-N_2-H_2O$ mixtures, both at a water vapor partial pressure of 2.3 kPa, were 6535 and 6169 K, respectively. The vibration temperature of the $CO-N_2-H_2O$ mixture with a water vapor partial pressure of 12.3 kPa with the addition of xenon was 5194 K. The vibration temperature of the $NH_3-CH_4-H_2-H_2O$ mixture, with a water vapor partial pressure of 12.3 kPa, was 8050 K.

The temperatures determined here by the analysis of the optical spectra emitted by large laser sparks are very close to the values reported in the literature[8,49−52] for LIDB with low-energy pulses provided by high-repetition lasers. There are no dramatic differences in plasma characteristics in these two cases when the LIDB plasma is expanding, interacting with a surrounding gas. However, different volumes of the chemically active plasma represent the main difference, leading to different total amounts of the products formed in a single laser shot.

This experiment with the pulse jet permitted direct investigation of the hot core of the LIDB plasma, excluding a role of

surrounding cold gas. The spectra obtained confirmed the expected strong emission in the extreme ultraviolet and soft X-ray regions. A spectrometer with a transmission grating was employed to record the spectra of multiple-charged ions of carbon, nitrogen, and oxygen to hydrogen-like ions, containing only one electron in their electron shells. The emission spectrum in the visible region was also studied in this experiment. No molecular bands were identified there. In conclusion, the presence of the cold molecular gas surrounding the hot core of the LIDB plasma is a necessary condition for formation of complex molecular species.

Acknowledgment. This work was funded by the Grant Agency of the Czech Republic, Grant No. 203/06/1278. During our experiments, the PALS facility was operated with a partial financial support of the Czech Ministry of Education, Grant LC528.

Supporting Information Available: Tables showing the assignment of emission lines in CO, H_2O, $CO-N_2-H_2O$ mixture, $CO_2-N_2-H_2O$ mixture, and $NH_3-CH_4-H_2-H_2O$ mixture LIDB plasma. This material is available free of charge via the Internet at http://pubs.acs.org.

References and Notes

(1) Miller, S. L. *J. Am. Chem. Soc.* **1955**, *77*, 2351.
(2) Schlesinger, G.; Miller, S. L. *J. Mol. Evol.* **1983**, *19*, 376.
(3) Miyakawa, S.; Sawaoka, A. B.; Ushio, K.; Kobayashi, K. *J. Appl. Phys.* **1999**, *85*, 6853.
(4) Scattergood, T. W.; McKay, C. P.; Borucki, W. J.; Giver, L. P.; Van Ghyseghem, H.; Parris, J.; Miller, S. L. *Icarus* **1989**, *81*, 413.
(5) Davis, D. D.; Smith, G. R.; Guillory, W. A. *Origins Life* **1980**, *10*, 237.
(6) McKay, C. P.; Borucki, W. J. *Science* **1997**, *276*, 390.
(7) Civiš, S.; Juha, L.; Babánková, D.; Cvačka, J.; Frank, O.; Jehlička, J.; Králiková, B.; Krása, J.; Kubát, P.; Muck, A.; Pfeifer, M.; Skála, J.; Ullschmied, J. *Chem. Phys. Lett.* **2004**, *386*, 169.
(8) Jebens, D. S.; Lakkaraju, H. S.; McKay, C. P.; Borucki, W. J. *Geophys. Res. Lett.* **1992**, *19*, 273.
(9) Chyba, C.; Sagan, C. *Origins Life Evol. Biosphere* **1991**, *21*, 3.
(10) Chyba, C.; Sagan, C. *Nature* **1992**, *355*, 125.
(11) Richter, J. In *Plasma Diagnostics*; Lochte-Holtgreven, W., Ed.; North-Holland: Amsterdam, 1968.
(12) Hutchinson, H. I. *Principles of Plasma Diagnostics*, 2nd ed.; Cambridge University Press: Cambridge, 1992.
(13) Griem, H. R. *Principles of Plasma Spectroscopy*; Cambridge University Press: Cambridge, 1997.
(14) Röpcke, J.; Davies, F. B.; Käning, M.; Lavrov, B. P. In *Low-Temperature Plasma Physics*; Hippler, R., Pfau, S., Schmidt, M., Schoenbach, K. H., Eds.; Wiley-VCH: Berlin, 2001; pp 173−197.
(15) Adelman, A. H. *J. Chem. Phys.* **1966**, *45*, 3152.
(16) Langsam, Y.; Ronn, A. M. *Chem. Phys.* **1981**, *54*, 277.
(17) Schwebel, A. H.; Ronn, A. M. *Chem. Phys. Lett.* **1983**, *100*, 178.
(18) Kielkopf, J. F. *Phys. Rev. E* **1995**, *52*, 2013.
(19) Fu, G. S.; Yu, W.; Li, X. W.; Han, L.; Zhang, L. S. *Phys. Rev. E* **1995**, *52*, 5304.
(20) Jungwirth, K.; Cejnarova, A.; Juha, L.; Kralikova, B.; Krasa, J.; Krousky, E.; Krupickova, P.; Laska, L.; Masek, K.; Mocek, T.; Pfeifer, M.; Präg, A.; Renner, O.; Rohlena, K.; Rus, B.; Skala, J.; Straka, P.; Ullschmied, J. *Phys. Plasmas* **2001**, *8*, 2495.
(21) Fiedorowicz, H.; Bartnik, A.; Juha, L.; Jungwirth, K.; Kralikova, B.; Krasa, J.; Kubat, P.; Pfeifer, M.; Pina, L.; Prchal, P.; Rohlena, K.; Skala, J.; Ullschmied, J.; Horvath, M.; Wawer, J. *J. Alloys Compd.* **2004**, *362*, 67.
(22) Pearse, R. W. B.; Gaydon, A. G. *The Identification of Molecular Spectra*; Wiley & Sons: New York, 1963.
(23) Wallaart, H. L.; Piar, B.; Perrin, M. Y.; Martin, J. P. *Chem. Phys. Lett.* **1995**, *246*, 587.
(24) Arepalli, S.; Scott, C. D.; Nikolaev, P.; Smalley, R. E. *Chem. Phys. Lett.* **2000**, *320*, 26.
(25) Voevodin, A. A.; Jones, J. G.; Zabinski, J. S. *J. Appl. Phys.* **2002**, *92*, 724.
(26) Keszler, A. M.; Nemes, L. *J. Mol. Struct.* **2004**, *695*−*696*, 211.
(27) Arepalli, S.; Scott, C. D. *Chem. Phys. Lett.* **1999**, *302*, 139.
(28) Rohlfing, E. A. *J. Chem. Phys.* **1988**, *89*, 6103.
(29) Neogi, A.; Narayan, V.; Thareja, R. K. *Phys. Lett. A* **1999**, *258*, 135.
(30) Marr, G. V. *Can. J. Phys.* **1957**, *35*, 1275.
(31) Kiess, N. H.; Bass, A. M. *J. Chem. Phys.* **1954**, *22*, 569.
(32) Janča, J. Folia Facultatis Scientiarum Naturalium Universitatis Purkynianae Brunensis. *Physica* **1973**, *14*, 109.
(33) Janča, J. *Czech. J. Phys. B* **1965**, *15*, 662.
(34) Pellerin, S.; Musiol, K.; Moret, O.; Pokrzywka, B.; Chapelle, J. *J. Phys. D* **1996**, *29*, 2850.
(35) Luque, J.; Crosley, D. R. *LIFBASE: Database and Spectral Simulation Program*, version 1.5; SRI International Report MP 99-009, 1999.
(36) Dick, K. A.; Benesch, W. *J. Mol. Spectrosc.* **1979**, *74*, 435.
(37) Mortet, V.; Hubička, Z.; Vorlíček, V. *Phys. Status Solidi A* **2004**, *201*, 2425.
(38) Liu, D.; Xu, Y.; Yang, X.; Yu, S.; Sun, Q.; Zhu, A.; Ma, T. *Diamond Relat. Mater.* **2002**, *11*, 1491.
(39) Voevodin, A. A.; Jones, J. G.; Zabinski, J. S. *J. Appl. Phys.* **2002**, *92*, 724.
(40) Tawde, N. R.; Trivedi, S. A. *Proc. Phys. Soc., London* **1939**, *51*, 733.
(41) Pillow, M. E. *Proc. Phys. Soc., London, Sect. A* **1953**, *66*, 737.
(42) Riascos, H.; Zambrano, G.; Prieto, P. *Braz. J. Phys.* **2004**, *34*, 1583.
(43) Fiedorowicz, H.; Bartnik, A.; Daido, H.; Choi, I. W.; Suzuki, M.; Yamagami, S. *Opt. Commun.* **2000**, *184*, 161.
(44) Chameides, W. L.; Walker, J. C. G. *Origins Life* **1981**, *11*, 291.
(45) Torres, J.; Jonkers, J.; van de Sande, M. J.; van der Mullen, J. J. A. M.; Gamero, A.; Sola, A. *J. Phys. D: Appl. Phys.* **2003**, *36*, L55.
(46) Goktas, H.; Demir, A.; Hajiyev, E.; Turan, R.; Seyhan, A.; Oke, G. *Int. Conf. Plasma* **2003**, *81*.
(47) Bekefi, G. *Principles of Laser Plasmas*; Wiley: New York, 1976.
(48) McWhirter, R. W. P. In *Plasma Diagnostic Techniques*; Huddlestone, R. H., Leonard, S. L., Eds.; Academic: New York, 1965.
(49) Alam, R. C.; Fletcher, S. S.; Wasserman, K. R.; Huwel, L. *Phys. Rev. A* **1990**, *42*, 383.
(50) Hornkohl, J. O.; Parigger, C.; Lewis, J. W. L. *J. Quant. Spectrosc. Radiat. Transfer* **1991**, *46*, 405.
(51) Simeonsson, J. B.; Miziolek, A. W. *Appl. Opt.* **1993**, *32*, 939.
(52) Villagrán-Muniz, M.; Sobral, H.; Navarro-González, R.; Velázquez, P. F.; Raga, A. C. *Plasma Phys. Controlled Fusion* **2003**, *45*, 571.